Sources of Distortion Study during Quench Hardening using Computer Modeling

Zhichao (Charlie) Li, B. Lynn Ferguson, Justin Sims, and Tianyu Yu
DANTE Solutions, Inc., 7261 Engle Road, Suite 105, Cleveland, OH 44130, USA

Abstract

Quench hardening is a transient thermal stress process with phase transformations. It is inevitable that a component will go through plastic deformation due to phase transformations, which will lead to distortion in the hardened part. Understanding the sources of distortion is necessary in designing the heat treat process and component configuration to obtain a product with greater dimensional accuracy. It is worth mentioning that consistent distortion can be compensated by adjusting the part dimensions prior to hardening. The possible sources of distortion include residual stresses prior to hardening, heating rate, austenitizing temperature, soaking time, quenching rate and uniformity, and possible tooling constraints, etc. The significance of these effects varies according to the part geometry and heat treatment process. Characterization of material properties and the development of computer modeling made it possible to understand the material and component responses during quench hardening, which is the key to process improvement and part configuration optimization. In this paper, the hardening process of a simplified bevel gear with thin-wall feature made of AISI 9310 is analyzed using DANTE, and the effect of tooling used in a press quench on distortion is investigated. The causes of distortion are analyzed through the material response aspect using the modeling results.

Introduction

Quench hardening is used to harden steel components through phase transformations. High hardness and strength properties are important to the fatigue performance of many steel components. Carburizing and quench hardening can generate beneficial compressive residual stresses in the hardened case due to the delayed martensitic transformation in the high carbon case. A post-machining (grinding) of the carburized case can damage the uniformity of the case, as well as the beneficial compressive residual stresses. Therefore, understanding the sources of distortion and controlling it during the quench hardening process are necessary.

During quenching, stresses caused by the thermal gradient and phase transformations create plastic strain in the part, which will cause distortion. A maximum amount of distortion caused by hardening is often specified for quality control, and parts with distortion exceeding the limit will be scrapped or reworked. Press quenching is one effective approach to reduce the distortion of parts with large size or complex geometry.

Quench hardening is a transient thermal stress process, the main sources of distortion include the thermal stresses and phase transformation stresses during both heating and cooling. Phase transformations make the quench hardening process highly nonlinear due to the changes of the thermal properties, mechanical properties, and density of the material, and it is difficult to investigate the sources of distortion through experiments. Heat treatment results that are of common interest include the volume fractions of phases, hardness, residual stresses, and dimensional change. The development of heat treatment simulation software makes it possible to understand the material response during the heat treatment process, including the evolution of internal stresses and deformation, the phase transformation sequences, and the probability of cracking. Computer simulation has increased the level of understanding of heat treatment processes because the events that occur during heating and cooling can be accurately modeled. In turn, advances in computer hardware, in combination with accurate simulation, have made the design and optimization of heat treatment processes more cost effective than traditional trial-and-error methods. DANTE is a coupled thermal, carbon diffusion, phase transformation and solid mechanics finite element based program for simulating the heat treatment of steel parts [1,2]. DANTE material models link with either ABAQUS Standard or ANSYS Mechanical solvers. Modeling results include the residual stress state after hardening, the evolution and final volume fractions of metallurgical phases, hardness, and part distortion. DANTE can be used to model austenitizing, gas carburizing, low pressure carburizing, immersion quench, high pressure gas quench, spray quench, induction hardening, press/plug quench, and tempering processes.

Phase Transformation Models

Quench hardening is a highly nonlinear process due to the phase transformations, and the accuracy of the phase transformation models is critical to the modeling results. The diffusive and martensitic transformation models in DANTE are described in equations (1) and (2) below.

$$\frac{d\Phi_d}{dt} = \nu_d(T)\Phi_d{}^{\alpha 1}(1-\Phi_d)^{\beta 1}\Phi_a \qquad (1)$$

$$\frac{d\Phi_m}{dT} = \nu_m(1-\Phi_m)^{\alpha 2}(\Phi_m+\varphi\Phi_d)^{\beta 2}\Phi_a \qquad (2)$$

where Φ_d and Φ_m are the volume fractions of individual diffusive phase and martensite transformed from austenite; Φ_a is the volume fraction of austenite; ν_d and ν_m are the mobilities of tranformation products, $\alpha 1$ and $\beta 1$ are material related

constants of diffusive transformation; $\alpha2$, $\beta2$ and φ are constants of martensitic transformation. For each individual phase formation, one set of transformation kinetics parameters is required.

Dilatometry data are often used to describe the phase transformation behavior of steels. Figure 1(a) is a continuous cooling dilatometry strain curve generated from the DANTE database representing the austenite to martensite transformation in AISI 9310. The horizontal axis in Figure 1(a) is temperature, and the vertical axis is the strain caused by temperature change and phase transformation. The strain change due to martensitic transformation is clearly quantified by the dialtometry experiments.

(a)

(b)
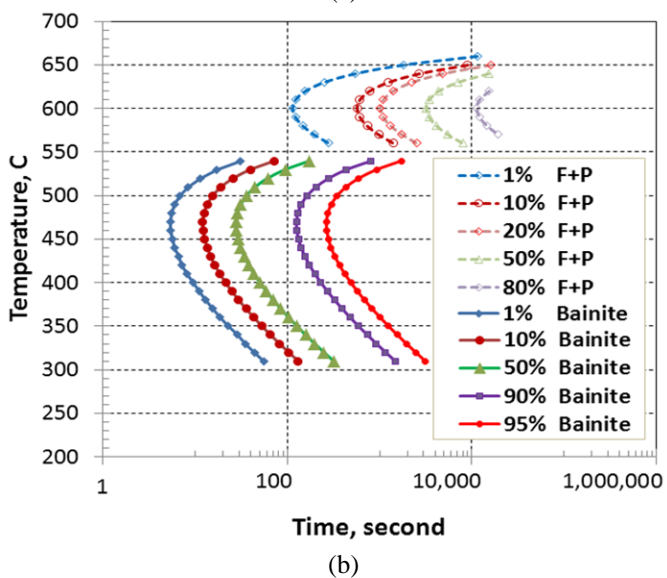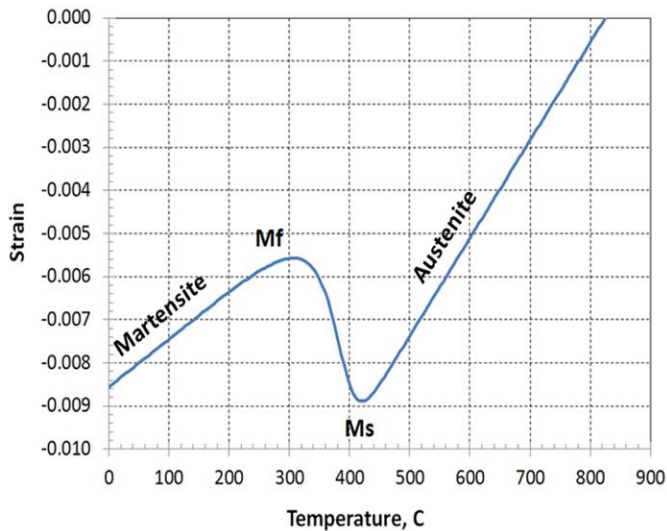
Figure 1. (a) Dilatometry strain curve with martensitic transformation, and b) TTT diagram of diffusive transformation for AISI 9310 steel.

When a dilatometry test sample cools below the martensitic transformation start (Ms) temperature, its volume expands with the crystal strucure change from austenite's face centered cubic (FCC) lattice to martensite's body centered tetragonal (BCT)

lattice. As known, the martensite's BCT structure has a lower density than austenite's FCC structure. The strain change in Figure 1(a) during transformation is a combination of thermal shrinkage and phase transformation expansion. The data obtained from this specific type of dilatometry test include coefficient of thermal expansion (CTE) for austenite and martensite, martensitic transformation starting (Ms) and martensitic transformation finishing (Mf) temperatures, transformation strain, and phase transformation kinetics (transformation rate) from austenite to martensite. These data are critical to the accuracy of modeling the internal stress and deformation caused by quenching.

Diffusive transformations are also characterized by dilatometry tests. A series of dilatometry tests with different cooling rates can be used to fit a full set of diffusive and martensitic phase transformation kinetics parameters. Once the full set of phase transformation kinetics paratmeters are fit from dilatometry tests, isothermal transformation (TTT) and continuous cooling transformation (CCT) diagrams can be generated for users to review. TTT/CCT diagrams are not directly used by DANTE phase transformation kinetics models, but they are useful because users can see the hardenability of the material graphically. Figure 1(b) is an isothermal transformation diagram (TTT) for AISI 9310 steel created from the DANTE database. To model the carburization and quench hardening processes of steel parts, properties of both the base carbon and high carbon material properies are required.

Description of Gear Geometry, Finite Element Model and Heat Treatment Processes

A simplified thin-wall bevel gear is used in this study. The CAD model of the gear is shown in Figure 2(a). The inner diameter of the gear is 78.0 mm, the height is 100.0 mm, and the outer diameter of tapered bevel tooth section is 100.0 mm. The thickness of the upper wall is 7.0 mm, and the thickness of the lower wall is 5.0 mm. This gear geometry is selected because of its tendency for large distortion during quenching hardening, mainly due to its stepped thin-wall and bevel tooth section. The gear material is AISI 9310, and a portion of the inner wall surface is selectively carburized, as shown in Figure 2(b). The out-of-round, straightness, and size of the gear wall are the main distortion modes. It is expected that the bevel tooth section will affect the straightness and radial size distortion. The bevel teeth are not modeled to simplify the model geometry, but the conical angle of the tooth tip surface is kept to more accurately catch the top die load effect during press quench. After removing the bevel teeth, the volume of the simplified model is kept the same as that of the original model by adjusting the conical surface position. For press quench using either expander or plug tooling design, the out-of-round distortion can be controlled effectively, but the radial distortion is difficult to control. Two-dimensional axisymmetric model can be used to predict the radial distortion including the straightness and the radial size effectively. In this study, one axisymmetric cross-section of the gear is used to model the gear response during quench hardening, and the finite element mesh is shown in Figure 2(b).

The FEA model includes 3,659 nodes and 3,468 4-node linear elements. Fine elements are used in the part surface to catch the steep gradients of carbon, temperature, phase transformation and stress evolutions during the entire hardening process.

(a)   (b)
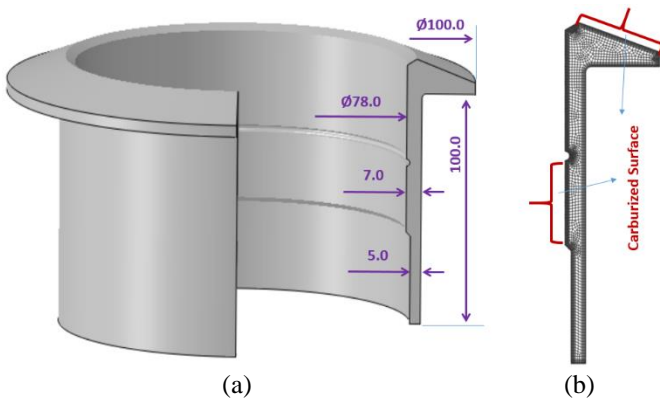
Figure 2. Simplified thin-wall bevel gear. a) CAD model and dimensions, and b) Finite element mesh.

Process Modeling of Gas Carburization and Immersion Oil Quench

The gear is gas carburized, followed by reheat and quench hardening. The bevel tooth surface and the middle section of the bore surface are carburized selectively, as shown in Figure 2(b). A two-step carburization process is used for this part. The first step is a boost step: with the temperature being 925° C, the carbon potential being 0.9%, and the time duration being 14400 seconds. The second step is the diffusion step: with the temperature dropping down to 875° C, the carbon potential being 0.8%, and the time duration being 7200 seconds. The predicted case depth is approximately 0.75 mm, and the predicted carbon distribution in terms of depth is shown in Figure 3.
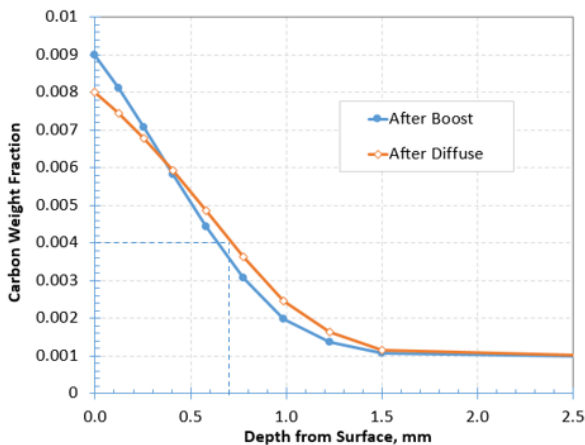
Figure 3. Carbon distributions in terms of depth after the boost and diffusion steps.

After carburization, the gear is slowly cooled to room temperature, followed by reheat for hardening. In this study, the residual stresses and distortion from the carburization process are ignored. The reheat temperature is 850° C, and the total

heating time is 1800 seconds including soaking with the assumption that all the carbides are dissolved into the iron matrix. After heating, the gear is transferred from the furnace to the quenching equipment in 10 seconds. The quench oil temperature is 65° C, and the total quenching time is 300 seconds, which is long enough to cool the gear to the oil temperature. After quenching, the gear is taken out and cooled to room temperature. To better understand the tooling effect during the press quench, an immersion oil quench without any mechanical tooling constraint is modeled first. The same thermal boundary conditions are used to model both the immersion and the press quench. The models also assume a uniform thermal boundary condition on the entire part surface.

During heating, the initial phases of the gear transform to austenite when the material is above the austenitizing transformation temperature. The temperature distribution in the part varies during heating due to its nonuniform wall thickness and the thicker bevel tooth section. Figure 4(a) shows the temperature, austenite and radial displacement distributions at 422.6 second during heating. The highest temperature of the part is slightly below the austenitizing temperature, so the internal stresses are caused purely by the temperature gradient. The predicted radial displacement is from the thermal expansion. The predicted radial displacement in Figure 4(e) shows more radial growth at the lower portion of the gear wall where the temperature is higher. The outer end of the bevel tooth has the largest radial displacements due to its radial size. Axial displacement is relatively uniform. The carburized case is in compression, which is caused by the higher coefficient of thermal expansion due to its higher carbon content.

(a)   (b)   (c)   (d)   (e)   (f)
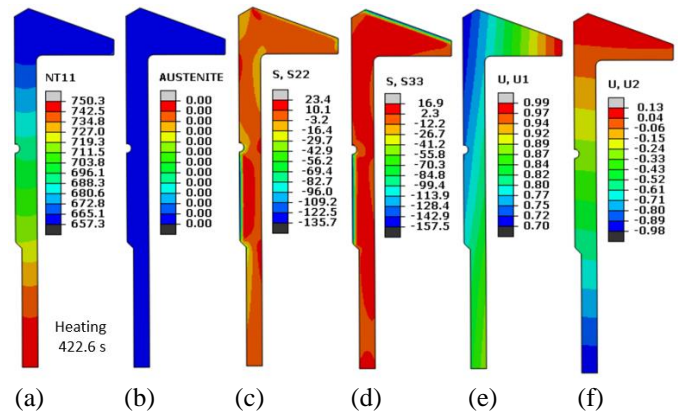
Figure 4. Modeling results during heating at 422.6 seconds. a) temperature, b) austenite, c) axial stress, d) circumferential stress, e) radial displacement, and f) axial displacement.

At 537.7 seconds during heating, the temperature at the lower portion of the wall reaches to 797° C, and the transformation to austenite occurs, as shown in Figure 5. With the transformation to austenite, the material volume shrinks, and the radial displacement of the lower portion of the wall is reduced from 0.8 mm before the austenite transformation starts to 0.6 mm when transformation occurs even though the temperature increased from 750° C to 797° C. With further heating, the temperature distribution of the middle axial section of the gear wall exceeds the austenite transformation temperature, and radial shrinkage occurs with the transformation. Phase

transformation to austenite also affects the stresses. The carburized case has a slightly earlier transformation to austenite, and the delayed transformation under the case will create a tensile stress as shown in Figures 5(c) and 5(d).

(a)   (b)   (c)   (d)   (e)   (f)
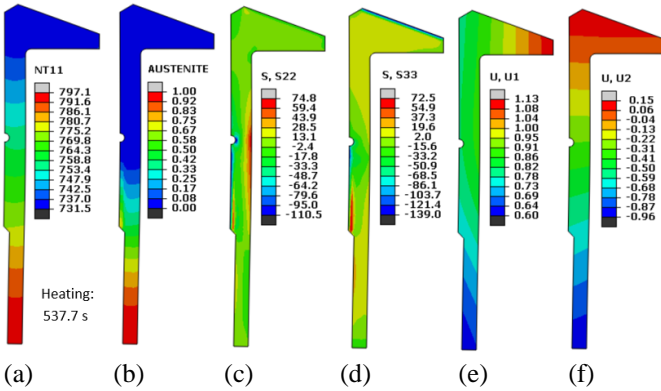
Figure 5. Modeling results during heating at 537.7 seconds. a) temperature, b) austenite, c) axial stress, d) circumferential stress, e) radial displacement, and f) axial displacement.

After the entire gear reaches to about 850° C, transformation to austenite has been completed, and the radial displacement of the wall is relatively uniform, as shown in Figure 6(e). The heating rate in this case is carefully controlled, and the stresses caused by the thermal gradient and phase transformation during heating are low enough to avoid excessive distortion. However, excessive distortion may occur in heat treatment practice with a high heating or austenitizing rate, especially for parts with large section thickness variation [3]. Stepped heating can be used to obtain more uniform temperature in the part when phase transformation to austenite occurs, which is an effective method to control the distortion caused by heating.

(a)   (b)   (c)   (d)   (e)   (f)
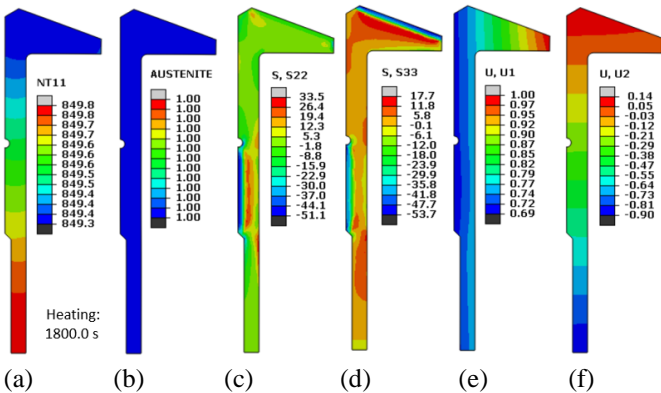
Figure 6. Modeling results at the end of heating. a) temperature, b) austenite, c) axial stress, d) circumferential stress, e) radial displacement, and f) axial displacement.

To more clearly analyze the effect of temperature and austenitic phase transformation on the radial displacement, a line of nodes located on the OD surface of the gear wall are selected for postprocessing, as shown in Figure 7(b). At the beginning of the heating, the radial displacements of all nodes are 0.0 mm, and they are perfectly straight. At 211.8 seconds, the lower portion of the gear wall has a higher temperature due to its thinner wall thickness, and the gear wall has a significant taper due the uneven thermal expansion. With further heating at 431.0

seconds, both the lower and upper portion of the wall are heated further without phase transformation. The temperature difference between the lower and upper portion of the wall doesn't change much from the snapshot at 211.8 seconds, so the gear wall has a further thermal expansion without much change on the taper magnitude. At 530.0 seconds, phase transformation to austenite occurs first at the lower portion of the gear wall, and significant radial shrinkage is observed at shown by the yellow curve in Figure 7. The transformation moves from the lower portion of the gear wall to upper portion, and an hourglass curvature moves upward with the transformation. After the entire gear transforms to austenite, a small hourglass shape is predicted a shown.
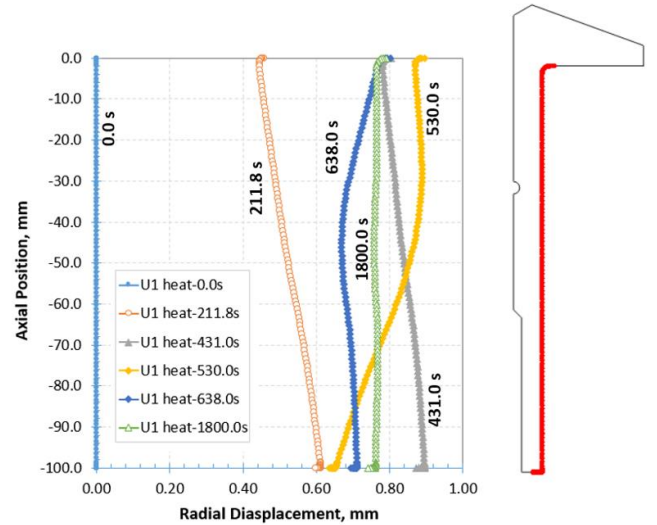
Figure 7. Effect of thermal expansion and austenitic phase transformation on the radial displacement of the gear wall during heating.

After heating, the gear is taken out of the heating furnace to quench using oil, and the transfer time is 10 seconds. The predicted temperature, phase, stresses, and displacements are shown in Figure 8. There is no phase transformation during the transfer time, and the thermal gradient is relatively small, and the material is in the elastic range. The lower portion of the gear wall has more thermal shrinkage radially due to its thinner wall thickness.

(a)   (b)   (c)   (d)   (e)   (f)
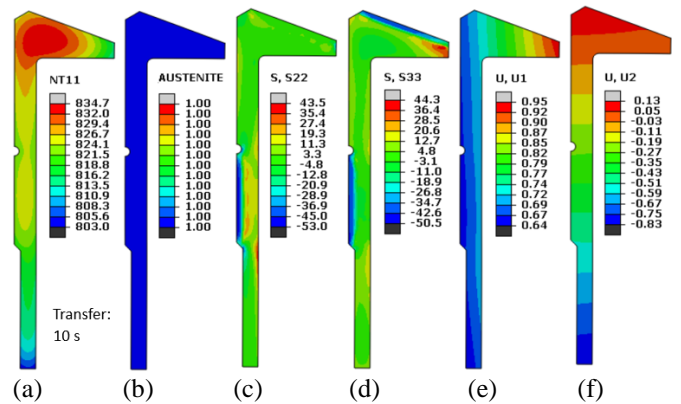
Figure 8. Modeling results at the end of the 10 second air transfer step. a) temperature, b) austenite, c) axial stress, d) circumferential stress, e) radial displacement, and f) axial displacement.

The martensitic transformation starting temperature is about 400° C for AISI 9310 base carbon steel, as shown in Figure 1(a). The internal stresses caused by the temperature gradient and phase transformations during quenching are much higher than those of the heating process, which is why the distortion caused by quenching is more than that of heating. At 2.0 seconds of quenching, the bottom of the gear wall has cooled to about 400° C (Ms), and the martensitic transformation is about to start. Prior to this point, the internal stresses in the part are caused purely by the temperature gradient. With a lower temperature at the bottom of the wall, its radial displacement decreases to 0.01 mm from the 0.7 mm at the end of the heating process, as shown in Figure 9(e). The radial displacement at the top of the wall is about 0.4 mm.

(a)   (b)   (c)   (d)   (e)   (f)
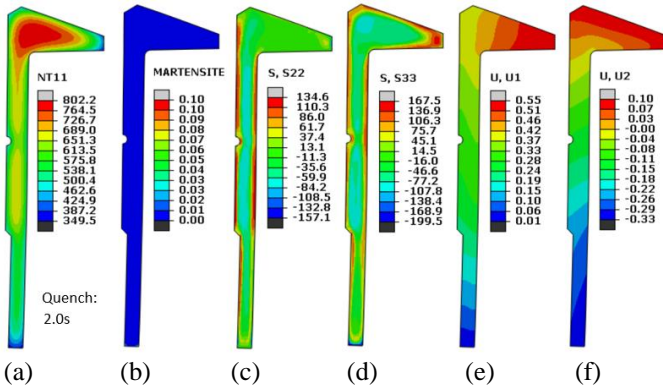
Figure 9. Modeling results at 2.0 seconds of immersion quench. a) temperature, b) martensite, c) axial stress, d) circumferential stress, e) radial displacement, and f) axial displacement.

With further cooling, the bottom of the gear wall drops to about 237° C at 7.8 seconds in quench, and the top is still above 350° C, as shown in Figure 10(a). The martensitic transformation in the lower portion of the wall is about 50%, while the upper portion is still mostly austenite. With martensitic transformation, the material expands, and the lower portion of the gear wall has a significant radial expansion, as shown in Figure 10(e).

(a)   (b)   (c)   (d)   (e)   (f)
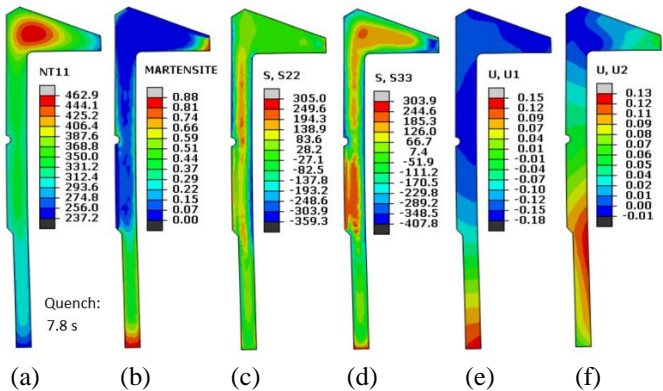
Figure 10. Modeling results at 7.8 seconds of immersion quench. a) temperature, b) martensite, c) axial stress, d) circumferential stress, e) radial displacement, and f) axial displacement.

The radial displacement is a combination of thermal shrinkage and volume expansion caused by the martensitic phase transformation during quenching. With further cooling, the martensitic transformation in the core of the thick bevel tooth section is completed, while the carburized case is still austenite due to its lower Ms temperature. The predicted radial displacement shows that the gear has a barrel shape at this moment, with positive radial displacement values. The carburized case transforms to martensite the latest, and the volume expansion by the martensitic phase transformation leads to compressive stresses in the case, which are balanced by tensile stresses in the core of the gear. Because the carburized case has a relatively small region, its delayed martensitic transformation has an insignificant effect on part distortion. Figures 11 and 12 are the predicted results after cooling the gear to the oil temperature and room temperature, respectively. Once the part cools to room temperature, the middle section of the wall has a radial displacement about +0.12 mm, the bottom is about 0.0 mm, and the top (bevel tooth section) is -0.09 mm.

(a)   (b)   (c)   (d)   (e)   (f)
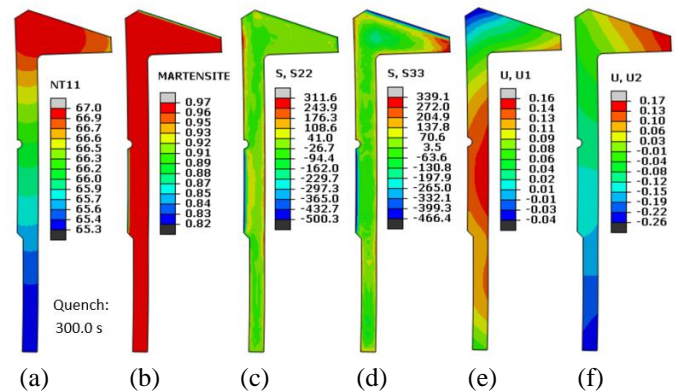
Figure 11. Modeling results after cooling the gear to the oil temperature using immersion quench. a) temperature, b) martensite, c) axial stress, d) circumferential stress, e) radial displacement, and f) axial displacement.

(a)   (b)   (c)   (d)   (e)   (f)
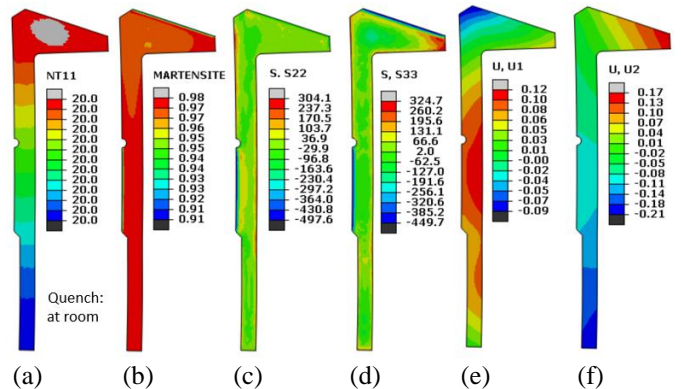
Figure 12. Modeling results after cooling the gear to room temperature using immersion quench. a) temperature, b) martensite, c) axial stress, d) circumferential stress, e) radial displacement, and f) axial displacement.

Using the same selected line of points selected in Figure 7, the radial displacements predicted at different times during quench are plotted in Figure 13. A small taper is predicted at the end of the 10 second transfer. At 2.0 seconds in quench, a significant taper is predicted, as shown in Figure 13 by the orange color

curve. With further cooling, the martensitic transformation at the bottom of the gear wall, and its radial displacement increases with the transformation. Both the thermal gradient and phase transformation will cause plastic strain in the part during oil quench in this case.
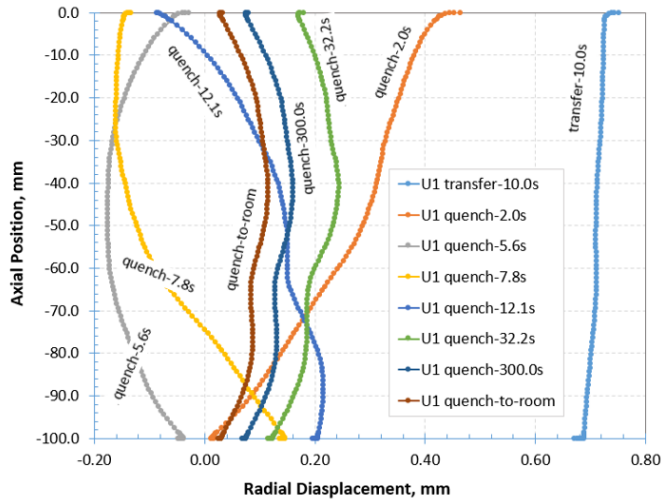
Figure 13. Effect of thermal shrinkage and martensitic phase transformation on the radial displacement of the gear wall during immersion quench process.

Press Quench Hardening Process

Press quenching has been used to control the distortion in this gear. The schematic press quench modeling set up is shown in Figure 14, with the assumption that the tooling components are rigid.
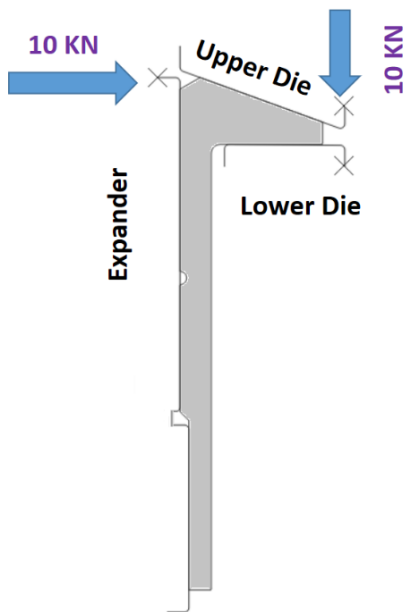
Figure 14. Schematic tooling set up for press quench process modeling.

A lower die is designed to hold the gear in the position, and 10 KN axial load is applied on the upper die to constrain the axial

warpage of the bevel tooth section. An expander is used to apply a radial load to the bore of the gear, and the expander can move in the radial direction. A 10 KN radial load is applied on the expander as shown.

Figure 15 shows the predicted results at 2.0 seconds during press quench, and the results have no significant difference from the immersion quench. In a press quench, the stresses generated by the applied external load should be much lower than the yield stress of the austenite at elevated temperature. If the load applied is too high, the distortion in the final part will not be consistent. However, a low expander load is still effective to control the out-of-round distortion because the applied radial load will be concentrated on the minor axial bore surface.
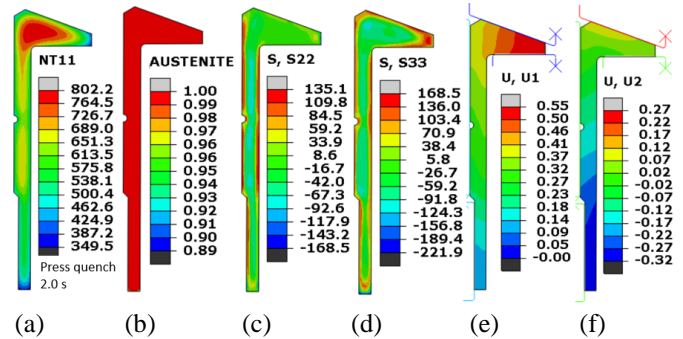
Figure 15. Modeling results at 2.0 seconds of press quench. a) temperature, b) martensite, c) axial stress, d) circumferential stress, e) radial displacement, and f) axial displacement.

When phase transformation occurs in the part, a localized phase transformation generates high internal stresses, which will put the material in a plastic deformation field. In this case, a low external load will contribute to plastic strain, and this phenomenon is called transformation induced plasticity (TRIP). The loads applied on the upper die and the expander are effective to constrain the distortion of gear due to the TRIP effect.
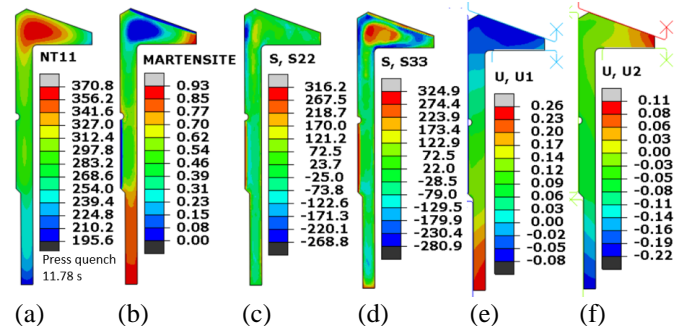
Figure 16. Modeling results at 11.78 seconds of press quench. a) temperature, b) martensite, c) axial stress, d) circumferential stress, e) radial displacement, and f) axial displacement.

Figure 17 shows the predicted results from press quench after cooling the gear to the room temperature. The residual stresses exhibit no significant difference compared to those of the immersion oil quench process. However, the bow distortion of the gear is reduced by press quench. With press quench, the axial displacement of the bevel tooth section is much more

uniform, as shown in Figure 17(f), comparing the immersion quenching results shown in Figure 12(f). The predicted axial expansion of the bevel tooth is about 0.05 mm, which is due the material density difference between the initial pearlite phase and the obtained martensite phase. In a heat treat process design, the material volume change should be considered.

(a)   (b)   (c)   (d)   (e)   (f)
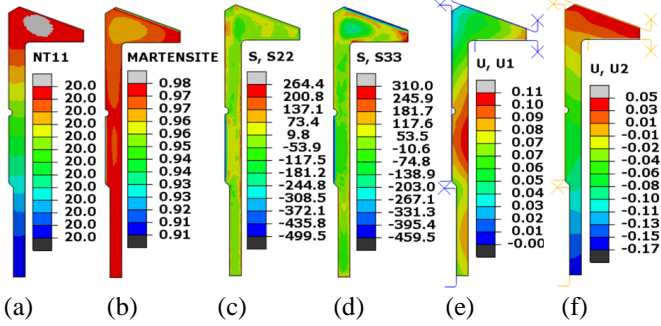
Figure 17. Modeling results after cooling the gear to room temperature using press quench. a) temperature, b) martensite, c) axial stress, d) circumferential stress, e) radial displacement, and f) axial displacement.

Using the same line of points as highlighted in Figure 7, the radial displacements of the gear wall are shown in Figure 18 at different times during press quench. Again, it is worth to mention that the tool loads applied are much lower than the material yield, and the external load will only be effective when phase transformation occurs in the part.
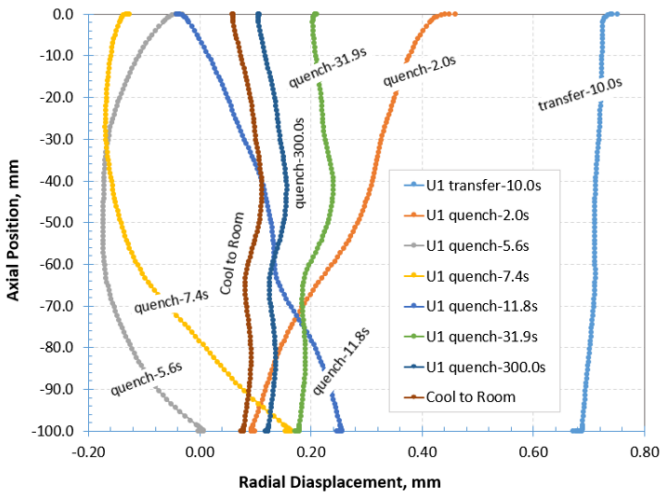
Figure 18. Effect of thermal shrinkage and martensitic phase transformation on the radial displacement of the gear wall during press quench process.

Figure 19 compares the predicted radial displacements of the gear wall between the immersion quench and the press quench using the highlighted points in Figure 7. The barrel shape is reduced approximately half.
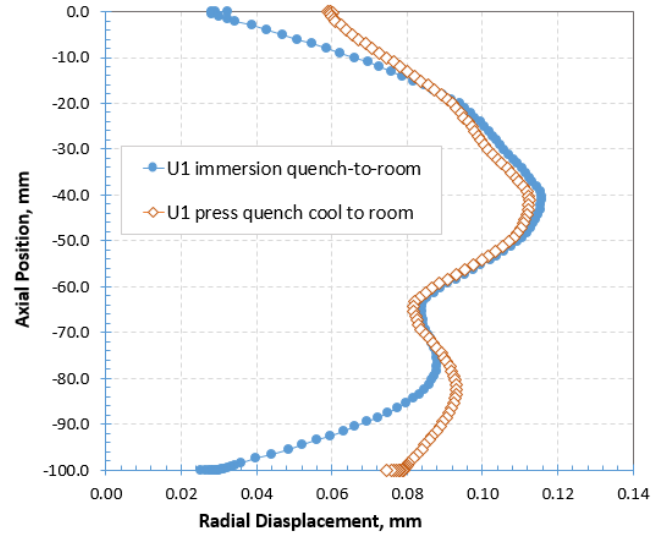
Figure 19. Comparison of predicted radial displacements of the gear wall between the press quench and immersion quench processes.

Conclusions

Using a simplified bevel tooth gear with thin-wall geometry, the quench hardening results between an immersion oil quench and a press quench are compared. The modeling results have clearly shown that the main sources of distortion are from the thermal stresses and phase transformation stresses. With phase transformations, the material will be in a plastic deformation field due to the localized volume change of the material, which will make the gear shape change permanently even with small external load. Because of this, the press quench can be effective with low applied load.

References

[1] B. L. Ferguson, A. Freborg, and G. Petrus, "Software Simulates Quenching", *Advanced Materials and Processes*, H31-H36, August (2000).

[2] D. Bammann, et al., "Development of a Carburizing and Quenching Simulation Tool: A Material Model for Carburizing Steels Undergoing Phase Transformations", *Proceedings of the 2nd International Conference on Quenching and the Control of Distortion,* 367-375, November (1996).

[3] Z. Li, B. L. Ferguson, and A. Freborg, "Data Needs for Modeling Heat Treatment of Steel Parts", *Proceedings of Materials Science & Technology Conference*, 219-226, (2004)